

1 **Novel Isothermal Membrane Distillation with**
2 **Acidic Collector for Selective and Energy-**
3 **Efficient Recovery of Ammonia from Urine**

4 Stephanie N. McCartney,[†] Natalie A. Williams,[†] Chanhee Boo,[†] Xi Chen[†] and
5 Ngai Yin Yip^{*,†,‡}

6 [†] Department of Earth and Environmental Engineering, Columbia University, New
7 York, New York 10027-6623, United States

8 [‡] Columbia Water Center, Columbia University, New York, New York 10027-6623,
9 United States

10 * Corresponding author: Email: n.y.yip@columbia.edu, Phone: +1 212 8542984

11 **ABSTRACT**

12 The high concentration of ammonia in source-separated urine offers propitious opportunities for
13 N recovery. Membrane distillation (MD) can recover volatile ammonia from hydrolyzed urine, but
14 conventional operation suffers from the simultaneous permeation of water vapor that results in
15 poor selectivity for ammonia transport and high energy demand. Here, we present a novel
16 operation of MD — *isothermal* membrane distillation with *acidic collector* (IMD-AC) — to
17 overcome the limitations of conventional MD. The innovative isothermal operation, i.e., same feed
18 and collector temperatures, effectively suppressed water vapor permeation while maintaining
19 ammonia vapor flux and, thus, significantly improved selectivity for ammonia transport. The
20 acidic collector further enhanced ammonia vapor flux by an average of 46.5% compared to using
21 a deionized water collector. Against a total ammoniacal nitrogen concentration gradient, i.e., uphill
22 transport, ammonia recovery of \approx 60% was attained, highlighting the prospect of the technology
23 for high-yield recovery. Critically, IMD-AC achieved approximately 95% savings in vaporization
24 energy consumption relative to conventional MD by practically eliminating the evaporation of
25 water. The resultant energy requirement of \approx 2.2 kWh/kg-N is less than the Haber-Bosch process
26 for N fixation and N removal by nitrification-denitrification (8.9-19.3 and 2.3-6.5 kWh/kg-N,
27 respectively). This study shows the promising potential of IMD-AC for the selective and energy-
28 efficient recovery of ammonia from source-separated urine.

29 **Keywords:** resource recovery, circular economy, waste utilization, low-grade heat, hydrophobic
30 microporous membrane, wastewater infrastructure

31 **INTRODUCTION**

32 Management of nitrogen, an essential nutrient for life, has been recognized by the National
33 Academy of Engineers as one of the Grand Challenges.¹ The current practices of N production,
34 consumption, and disposal are unsustainable.² Anthropogenic N emissions to the aquatic
35 ecosystem cause eutrophication, harmful algal blooms (HABs), and hypoxic dead zones in surface
36 waters and marine coastal areas.³⁻⁵ In addition to the ecological and environmental devastation,
37 cyanobacteria and algal toxins from HABs pose public health threats.^{6,7} Reducing N discharge
38 from point sources, such as wastewater treatment plant (WWTP) effluent, has been identified as a

39 vital nutrient contaminant management strategy.⁸ However, most WWTPs are not equipped with
40 tertiary treatment, i.e., dedicated stage for nutrient removal. Even when advanced treatment is
41 present to lower N concentrations, considerable energy and chemical costs are required.⁹
42 Conventional N removal by nitrification-denitrification at WWTPs demands 2.3-6.5 kWh/kg-N.¹⁰⁻
43 13

44 Global food security is dependent on ammonia, the bioavailable form of N and a principal
45 component of fertilizer. At the same time N is emitted to the environment, nitrogen is fixed from
46 the atmosphere through the energy-intensive Haber-Bosch process, requiring 8.9-19.3 kWh/kg-N,
47 and accounts for ≈1-2% of the world's energy use.¹⁴⁻¹⁶ In other words, ammonia is produced at
48 huge energy cost and further expenditures are incurred downstream, for the removal of excess
49 nutrients from our wastewater to prevent environmental and public health problems. The
50 biogeochemical flow of nitrogen is, hence, flagged as exceeding the safe operating space for
51 humanity, posing high risks under the planetary boundaries framework.² The current linear
52 economy approach is clearly untenable and a new paradigm for sustainable nitrogen management
53 is urgently needed.¹⁷⁻¹⁹

54 Instead, nitrogen in anthropogenic wastewaters can be recovered to promote a more
55 sensible circular economy model. Nitrogen recovery efforts at WWTPs are presently constrained
56 by pollution risks, low yields, and/or high costs. Land applications of biosolids, i.e., treated sewage
57 sludge, is the prevailing practice;^{20,21} however, the method risks contamination from toxic heavy
58 metals, pharmaceuticals, personal care products, and pathogens.²⁰⁻²⁶ Approaches that separate N
59 from WWTP wastewater for reuse were explored,²⁷⁻³² but progress is thwarted by low recovery
60 yields and high energy and chemical expenses of these techniques.³³ For instance, ammonia
61 recovery from wastewater by precipitation of phosphate-based minerals is typically limited to only
62 ≈5-15% yield,^{30,31} and energy demand of N recovery methods range from approximately 5 to 18
63 kWh per kg of N.^{10,30,34,35} An underlying reason for the difficulties in implementing practical N
64 harvesting at WWTPs is the inherently low nutrient concentration of the flows.

65 A more forward-looking approach that is better aligned with the principles of Green
66 Engineering is to recover N from source-separated urine,³⁶⁻³⁹ which contains ≈80% of the nitrogen
67 from human excretions.⁴⁰⁻⁴² Because urine isolated at-source is not diluted by flush water and grey
68 water, the N concentration is two orders of magnitude greater than municipal wastewater, a

69 significantly more favorable condition for separation and capture.^{37-39,41,43,44} Various approaches
70 to extract ammonia from urine have been explored, including vacuum distillation, stripping-
71 adsorption, mineral precipitation, ion-exchange, and electrochemical methods.⁴⁵⁻⁵¹ However, most
72 efforts thus far have generally fallen short of cost-competitiveness with the Haber-Bosch process
73 because the approaches were prohibitively capital-intensive and/or demanded high operating
74 energy and chemical cost.^{10,39,46,52,53}

75 Membrane distillation (MD), an emergent technology that utilizes low-temperature heat to
76 drive the permeation of volatile compounds across a hydrophobic microporous membrane,⁵⁴⁻⁵⁶ can
77 take advantage of the intrinsic high volatility of ammonia.⁵⁷⁻⁵⁹ Most MD studies focused on
78 desalination, i.e., separation of water from saline feed streams,^{54-56,60} but potential of the technique
79 for ammonia separation and recovery were recently investigated.^{57-59,61-80} However, harvesting
80 ammonia from source-separated urine using MD is hampered by the undiscerning transport of all
81 volatile components, including water. The unavoidable permeation of H₂O along with NH₃ is
82 undesirable because of the additional energy demand to evaporate water and dilution of the product
83 stream.^{61,62}

84 In this study, we demonstrate a novel operation of direct contact membrane distillation,
85 termed isothermal membrane distillation with acidic collector (IMD-AC) to overcome the
86 limitations of conventional MD in the separation and recovery of ammonia from simulated urine.
87 The working principles of IMD-AC are first presented and the features differentiating the
88 technique from conventional MD are highlighted. Vapor fluxes of ammonia and water in
89 conventional and isothermal MD are compared, and the selectivity for NH₃ permeation over H₂O
90 is analyzed. The influence of an acidic solution as the collector stream on NH_{3(g)} transport is
91 examined. Next, the study evaluated the effects of temperature on IMD-AC performance. Heat
92 energy consumed to vaporize water and ammonia is then quantified to assess the energy savings
93 of IMD-AC over conventional MD. The implications of IMD-AC for ammonia recovery from
94 source-separated urine are discussed, and the potential utilization for other environmental
95 applications are identified.

96 ISOTHERMAL MEMBRANE DISTILLATION WITH ACIDIC COLLECTOR

97 Limitations of Conventional Membrane Distillation for Ammonia Recovery.

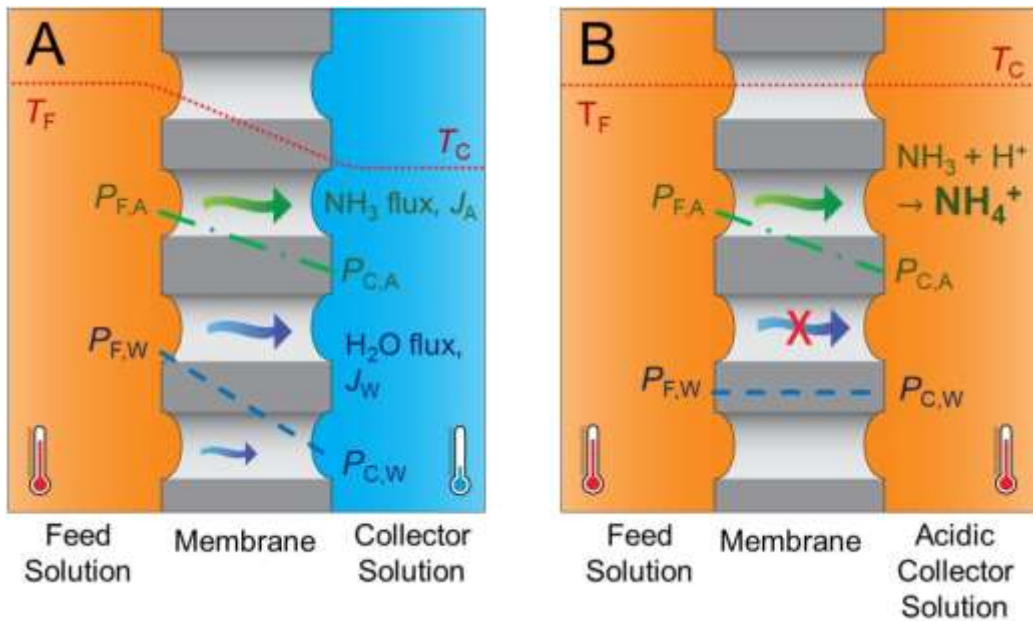
98 Membrane distillation (MD) is a separation process where volatile compounds are driven across a
99 hydrophobic microporous membrane while nonvolatile components are retained in the feed stream.
100 Working principles of MD are detailed in literature,^{54,55} and are briefly explained here with specific
101 focus on ammonia recovery. In the conventional operation of direct contact MD, the feed stream
102 is at a higher temperature than the permeate, or sweep/collector, stream, i.e., $T_F > T_C$ (subscripts F
103 and C denote feed and collector streams, respectively). Because partial vapor pressure of volatile
104 component i , P_i , is exponentially dependent on the solution temperature, as described by the
105 Clausius-Clapeyron relation,⁸¹ the temperature difference sets up a vapor pressure gradient
106 between the feed and collector sides at the solution-membrane interfaces. The transmembrane
107 vapor pressure difference, $P_{F,i} - P_{C,i}$ (subscripts F and C denote feed and collector sides,
108 respectively), is the driving force for the compound to volatilize from the feed solution, permeate
109 across the membrane, and eventually condense in the collector stream. Vapor flux of component
110 i , J_i , is described by eq 1:⁵⁵

$$111 \quad J_i = L_i (P_{F,i} - P_{C,i}) \quad (1)$$

112 where membrane vapor permeability coefficient, L_i , characterizes the transport of compound i per
113 unit driving force and is dependent on the vapor molecule, membrane structural properties and
114 membrane chemistry, feed and collector compositions, as well as operating conditions, such as
115 temperature.⁵⁴⁻⁵⁶

116 Although MD is primarily employed for water recovery from saline feed streams, i.e.,
117 desalination,^{54,55,82} the technique can also be used to separate volatile compounds, including
118 ammonia, from aqueous solutions.^{57-59,75,83} However, using conventional membrane distillation
119 (CMD) for ammonia separation also unavoidably also vaporizes water, resulting in simultaneous
120 permeation of water vapor together with $\text{NH}_3\text{(g)}$ flux (Figure 1A). The indiscriminate transport of
121 water limits the effectiveness of conventional MD in applications where selective permeation of
122 one volatile component is desired. For NH_3 recovery from urine, the incidental water vapor flux,
123 J_w , unfavorably dilutes the ammonia concentration of the product (i.e., collector stream effluent).⁸⁴
124 More importantly, because evaporating water is very energy intensive (enthalpy of vaporization

125 $\approx 630 \text{ kWh/m}^3$), the concomitant J_w would detrimentally raise the thermal energy input required
 126 for the overall process. Note that column distillation is similarly encumbered by the disadvantage
 127 of inevitable water evaporation.



128

129 **Figure 1.** Temperature and vapor pressure profiles for A) conventional and B) isothermal MD with
 130 acidic collector. The temperature difference between the solution-membrane interfaces in CMD
 131 establishes a water vapor pressure gradient from feed to collector side, thus driving water vapor flux,
 132 J_w (blue arrow). Whereas the driving force for J_w is effectively zero in IMD, because the identical
 133 solution temperatures set up a constant water vapor pressure across the membrane. As $\text{NH}_3(g)$ vapor
 134 pressure is linearly proportional to ammonia concentration in the aqueous solution (Henry's law), both
 135 CMD and IMD exhibit a gradient for ammonia vapor pressure from feed to collector side, thus driving
 136 $\text{NH}_3(g)$ permeation, J_A (green arrows). Permeated NH_3 that solubilizes in the acidic collector solution
 137 associates with H^+ to form nonvolatile NH_4^+ .

138 **Working Principles of Isothermal Membrane Distillation with Acidic Collector.**

139 To overcome the limitations of conventional MD for separating volatile compounds from aqueous
 140 solutions, specifically the recovery of ammonia from hydrolyzed urine, we introduce *isothermal*
 141 membrane distillation (IMD), where the feed and collector streams are at the same temperature,
 142 i.e., $T_F = T_C$. Note that the main form of nitrogen in fresh, i.e., unhydrolyzed urine, is urea,
 143 $\text{CO}(\text{NH}_2)_2$, which has a very low Henry's Law constant; urea undergoes hydrolysis by urease
 144 enzymes naturally present in urine to form bicarbonate and volatile ammonia, eventually yielding
 145 hydrolyzed urine,⁴¹ i.e., MD is not applicable to fresh urine for N recovery. The equivalent

146 temperature on both sides effectively eliminates the partial H_2O vapor pressure gradient, thus
147 ceasing the driving force for water vapor transport. Partial vapor pressure is linearly proportional
148 to concentration of the volatile component in aqueous solution, c_i , as governed by Henry's and
149 Raoult's laws (determination of vapor pressure of solutions of different composition and
150 temperature is detailed in the Supporting Information).⁸⁵ Therefore for ammonia (and other volatile
151 compounds), a driving force for permeation from feed to collector subsists for $c_{F,A} > c_{C,A}$ (subscript
152 A indicates ammonia, NH_3), even when temperature profile across the membrane is flat, i.e., unlike
153 conventional MD operation (Figure 1B). Critically, by curbing J_w , IMD avoids the heat energy
154 input required to evaporate water that is unpreventable in conventional MD.

155 In the isothermal operation of MD, ammonia vapor permeates from feed to collector side
156 when there is an $\text{NH}_{3(\text{aq})}$ concentration gradient between the aqueous solutions, i.e., $c_{F,A} - c_{C,A} > 0$.
157 But as more ammonia is separated from the feed stream and captured in the collector stream, $c_{F,A}$
158 decreases while $c_{C,A}$ increases, thus gradually diminishing the driving force for ammonia vapor
159 flux, J_A (eq 1). Eventually ammonia recovery ceases as $\text{NH}_{3(\text{aq})}$ concentration of the collector
160 approaches the feed solution. To address this constraint, a second feature of acidic collector (AC)
161 is incorporated to promote the speciation of volatile ammonia, NH_3 , in the collector stream to ionic
162 ammonium, NH_4^+ , which is nonvolatile.^{57,58,61-74} A weak acid in the collector solution maintains a
163 low pH that is below the $\text{p}K_A$ of ammonia (between 9.4 and 8.3 for solution temperatures of 20-
164 60 °C),⁸⁶ effectively converting all NH_3 that has permeated over to the collector to NH_4^+ (Figure
165 S1 of Supporting Information). Therefore, $\text{NH}_{3(\text{aq})}$ concentration of the collector stream is
166 practically negligible, i.e., $c_{C,A} \approx 0$, even though the total ammoniacal nitrogen, $\text{NH}_3 + \text{NH}_4^+$,
167 concentration increases. Therefore, a positive driving force for J_A is always sustained, i.e.,
168 $P_{F,A} - P_{C,A} > 0$. Overall, the isothermal and acidic collector features of IMD-AC can, respectively,
169 suppress the undesirable permeation of water vapor, thus reducing the heat energy required to
170 vaporize water, and eliminate the partial vapor pressure of ammonia in the collector solution, to
171 maximize the driving force for NH_3 flux and enable high recovery yields.

172 **EXPERIMENTAL SECTION**

173 **Materials and Chemicals.** Commercial microporous hydrophobic polyvinylidene fluoride
174 (PVDF) membrane of 0.22 μm pore-size, GVHP14250, was acquired from MilliporeSigma

175 (Burlington, MA) and utilized for all membrane distillation experiments. The simulated urine feed
176 solution comprised 250 mM ammonium hydroxide and 250 mM ammonium bicarbonate in
177 deionized (DI) water from a Milli-Q ultrapure water purification system (MilliporeSigma), to
178 mimic the total ammoniacal concentration and pH of hydrolyzed urine.^{37-39,41,42} DI water was used
179 for the collector stream in non-acidic MD experiments. To prepare the acidic collector solution,
180 acetic acid was diluted in DI water. All chemicals utilized in the experiments are analytical grade
181 and were purchased from ThermoFisher Scientific (Waltham, MA).

182 **Ammonia Separation and Recovery Experiments.** Ammonia and water vapor
183 fluxes were evaluated in four different operating modes: conventional membrane distillation with
184 DI water collector (CMD-DI), conventional MD with acidic collector (CMD-AC), isothermal MD
185 with DI water collector (IMD-DI), and isothermal MD with acidic collector (IMD-AC). I.e., the
186 parameters assessed are collector stream composition (DI water or acid) and conventional versus
187 isothermal operation. Simulated hydrolyzed urine was consistently utilized as the feed solution.
188 For CMD-AC and IMD-AC operations, 100 mM acetic acid was employed as the collector solution.
189 In the conventional MD experiments, a 20 °C temperature differential was applied, with the feed
190 and collector streams maintained at 40 and 20 °C, respectively. In the comparison analysis, the
191 feed and collector streams of isothermal MD were operated at the same temperature of 40 °C (i.e.,
192 same temperature as feed solution of CMD). To investigate the effect of temperature on
193 performance, IMD-AC was additionally operated with $T_F = T_C$ at 20, 30, 50, and 60 °C. Volume
194 of the feed and collector solutions are approximately 2.0 L each.

195 All experiments were conducted in a bench-scale MD unit (Figure S2 of Supporting
196 Information). The feed and collector streams were circulated countercurrently at crossflow
197 velocities of 22.2 cm/s and 20.0 cm/s, respectively, across the active membrane area of 19.0 cm²
198 in a custom-built membrane cell. T_F and T_C were regulated with heated and refrigerated circulators
199 (PolyScience, Warrington, PA), respectively, through heat exchangers. Temperatures at the inlet
200 and outlet of the membrane cell on the feed and collector sides were monitored using
201 thermocouples (Omega Engineering, Norwalk, CT) and the solution within the cell is maintained
202 within ± 1.5 °C of the target temperature throughout all experimental runs.

203 Ammonia vapor flux was determined from the rate of change of total ammoniacal nitrogen
204 (TAN = $\text{NH}_3 + \text{NH}_4^+$) in the collector stream. Four 1 mL samples were taken every 15 min, and

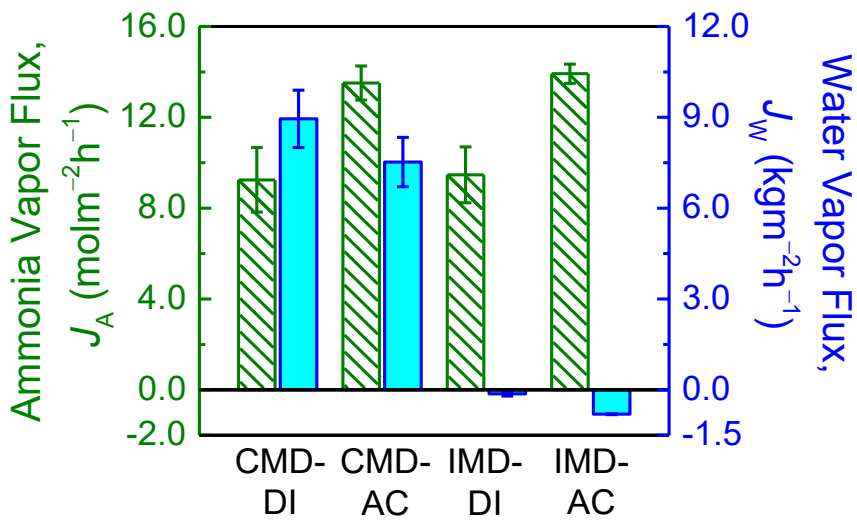
205 TAN concentrations were measured following the Indophenol blue method.⁸⁷ Ammonia salicylate
206 and ammonia cyanurate reagent powder were added in excess to DI water-diluted samples and
207 analyzed using a calibrated colorimeter (ThermoFisher Scientific). The change in moles of
208 ammonia over time normalized by the membrane area yields J_A . Additionally, pH of the collector
209 stream was measured during sampling with a pH Meter (Orion Star, ThermoFisher Scientific).
210 Water flux was calculated as the average rate of change in the feed and collector solution weights
211 normalized by membrane area, accounting for the transferred ammonia and evaporative loss from
212 bulk solution tanks. The change in weight of the feed and collector bulk solution tanks were
213 automatically logged every 10 seconds using digital microbalances (AX5202, Ohaus, Parsippany,
214 NJ).

215 To demonstrate the potential of IMD-AC for high-recovery of ammonia, an isothermal MD
216 experiment was conducted at 40 °C with the feed and collector solutions at the same initial
217 ammoniacal nitrogen concentration. The feed solution was simulated urine (i.e., 500 mM TAN),
218 while the collector solution composition was 750 mM acetic acid and 500 mM ammonium chloride
219 (a higher acetic acid concentration than the earlier described experiments was employed to ensure
220 collector stream pH was maintained sufficiently lower than the pK_a of ammonia throughout the
221 experiment duration). The experimental run was conducted for 6 h, with ammonia concentrations
222 in the collector stream measured every 1.5 h.

223 RESULTS AND DISCUSSION

224 **Higher Ammonia Selectivity is Achieved using Isothermal MD.** Figure 2 shows
225 ammonia and water vapor fluxes (green patterned columns, left vertical axis and blue solid
226 columns, right vertical axis respectively) under CMD and IMD operation with DI water and acidic
227 collector. For the same collector solution of DI water, J_A was practically consistent between
228 conventional and isothermal MD (9.25 $\text{mol m}^{-2} \text{h}^{-1}$ for CMD-DI and 9.47 $\text{mol m}^{-2} \text{h}^{-1}$ for IMD-DI).
229 At 40 °C, pH of the simulated urine feed solution is 8.8 whereas $pK_a = 8.8$ and, thus, volatile $\text{NH}_3(\text{aq})$
230 and NH_4^+ are of approximately equal concentrations (≈ 250 mM). Isothermal operation of direct
231 contact MD did not affect $\text{NH}_3(\text{g})$ transport as the driving force for ammonia vapor permeation,
232 $P_{\text{F},\text{A}} - P_{\text{C},\text{A}}$, is essentially equal for IMD and CMD (excluding temperature polarization effects,
233 which will be discussed later) because the feed composition and temperature were held constant

234 and ammonia concentration in the collector is negligible throughout the relatively short experiment
 235 duration. A comparison between CMD-AC and IMD-AC also presented minimal difference in J_A
 236 (13.5 and 13.9 $\text{molm}^{-2}\text{h}^{-1}$, respectively), further validating that ammonia vapor flux is not affected
 237 by warming the collector stream to T_F for isothermal MD operation. Effect of acidic collector on
 238 ammonia vapor fluxes is discussed in the next section.



239

240 **Figure 2.** Ammonia and water vapor fluxes for four different MD operations: CMD-DI with 40 °C feed
 241 and 20 °C DI water collector, CMD-AC with 40 °C feed and 20 °C acidic collector, IMD-DI with 40 °C
 242 feed and 40 °C DI water collector, and IMD-AC with 40 °C feed and 40 °C acidic collector. The feed
 243 stream for all scenarios is simulated solution of hydrolyzed urine (250 mM NH_4OH and 250 mM
 244 NH_4HCO_3), whereas acidic collector is 100 mM acetic acid. The green patterned columns correspond
 245 to ammonia vapor fluxes (left vertical axis) and the blue solid columns denote water vapor fluxes (right
 246 vertical axis). Error bars indicate standard deviations of duplicate experiments with different membrane
 247 coupons.

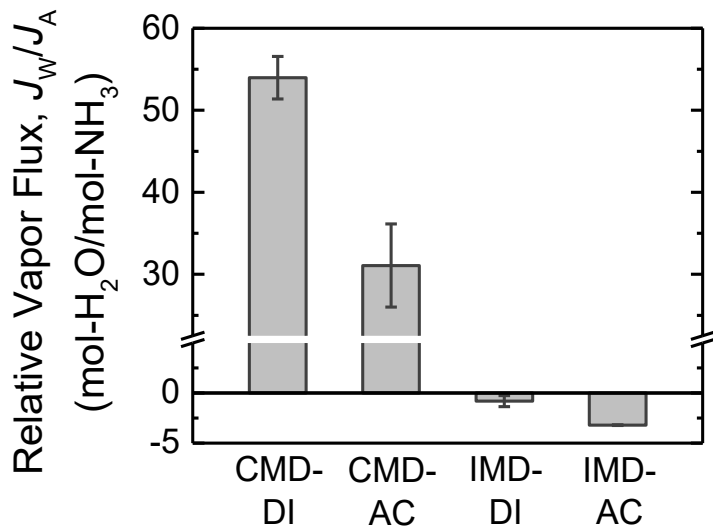
248 In contrast to ammonia vapor permeation, water vapor fluxes were drastically different
 249 between IMD and CMD operation. Under CMD operation, water flux in the direction of feed to
 250 collector was significant, measuring 8.9 and 7.5 $\text{kgm}^{-2}\text{h}^{-1}$ with DI water and acidic collector,
 251 respectively. The imposed 40-20 °C temperature differential in CMD set up a water vapor pressure
 252 gradient across the microporous membrane, which drove water vapor permeation from the feed to
 253 the collector side. On the other hand, J_W in IMD is markedly suppressed by over an order of
 254 magnitude to 0.13 and 0.80 $\text{kgm}^{-2}\text{h}^{-1}$ for DI water and acidic collector, respectively. Elevating T_C
 255 to match T_F in isothermal operation raised the water vapor pressure at the collector side to $\approx P_{F,W}$

256 (Figure 1B). Note that the effect of solution composition (i.e., DI water or 100 mM acetic acid) on
257 partial vapor pressure is negligible relative to the influence of temperature. The driving force for
258 J_w is, therefore, effectively eliminated in IMD-DI and IMD-AC, i.e., $P_{F,w} - P_{C,w} = 0$, and H_2O
259 transport was almost fully inhibited (eq 1).

260 Direction of the diminished J_w for IMD is opposite to CMD, i.e., water vapor permeated
261 from collector to feed side (indicated as negative fluxes in Figure 2). The reversed water vapor
262 flux is attributed to temperature polarization at the solution-membrane interfaces producing a
263 slight local transmembrane temperature gradient toward the feed side. In NH_3 transport, ammonia
264 volatilizes from the feed stream at the membrane interface, permeates across the membrane, and
265 solubilizes in the collector solution. These phase-changes necessary for NH_3 transport in MD
266 inevitably cools the feed and warms the collector solutions near the membrane surface, a
267 phenomenon termed temperature polarization.⁸⁸⁻⁹⁰ Hence, even though the bulk solution
268 temperatures are similar in IMD, there is a water vapor pressure gradient from collector to feed
269 side, i.e., $P_{C,w} > P_{F,w}$, yielding negative J_w (illustrated in Figure S3 of Supporting Information).
270 Temperature polarization likewise occurs in CMD, but the bulk solution temperature difference
271 overwhelms the local deviations. Thus, $P_F > P_C$ and water and ammonia vapor fluxes are always
272 positive, i.e., from feed to collector side.

273 For the separation and recovery of ammoniacal nitrogen from hydrolyzed urine, high
274 ammonia vapor permeation and minimal water vapor flux is desired to minimize energy required
275 for vaporization enthalpy and limit watering down of the product (i.e., collector stream effluent).
276 That is, selective transport of NH_3 over H_2O is advantageous. Figure 3 presents the relative molar
277 flux of water to ammonia for the four operating conditions, with a lower J_w/J_A signifying better
278 selectivity for ammonia transport. The magnitude of J_w/J_A for conventional operation is
279 significantly higher than the isothermal processes (negative values for IMD reflect the reversed
280 direction of water vapor permeation). For every mole of ammonia volatilized from the feed stream,
281 54 and 31 moles of water are simultaneously evaporated in CMD-DI and CMD-AC, respectively,
282 underscoring that thermal energy input for vaporization enthalpy is predominantly consumed for
283 H_2O and not the intended NH_3 (detailed energy analysis is presented in a later section). The poor
284 selectivity of CMD is attributed to the concentration of water being about 100 \times higher than
285 ammonia in the simulated urine stream (≈ 55.5 mol- H_2O/L compared to 0.5 mol- NH_3/L),
286 overwhelming the effect of greater volatility of ammonia than water. The transport of water in

287 isothermal MD was suppressed by up to 68 \times compared to conventional operation (-0.803 and
 288 -3.02 mol-H₂O/mol-NH₃ for IMD-DI and IMD-AC, respectively), highlighting the enhanced
 289 selectivity of IMD for ammonia separation and recovery. The relative vapor flux in kg-H₂O/mol-
 290 NH₃ is presented in Figure S4 of the Supporting Information.



291

292 **Figure 3.** Relative molar flux of water to ammonia for the four operations, CMD-DI, CMD-AC, IMD-
 293 DI, and IMD-AC. IMD-DI and IMD-AC exhibit negative relative fluxes because water vapor
 294 permeation was in opposite direction, from collector to feed side. Error bars indicate standard deviations
 295 of duplicate experiments with different membrane coupon.

296 **Acidic Collector Enhances Ammonia Vapor Flux.** Under acidic collector operation,
 297 CMD-AC and IMD-AC, ammonia vapor fluxes were, on average, 46.5% higher than with DI water,
 298 CMD-DI and IMD-DI (green patterned columns, left vertical axis of Figure 2). As ammonia
 299 permeates from feed to collector, pH of the collector rose above 10 when DI water is used, but
 300 remained below 4 with acetic acid as collector (Figure S5). At solution temperatures of 20 and
 301 40 °C, pK_A of NH_{3(aq)} is 9.4 and 8.8, respectively. Consequentially, ammoniacal nitrogen is
 302 predominantly in the form of ammonia, NH_{3(aq)}, in DI water collector, whereas ammonia
 303 protonates to nonvolatile ammonium, NH₄⁺, in the acidic collectors.

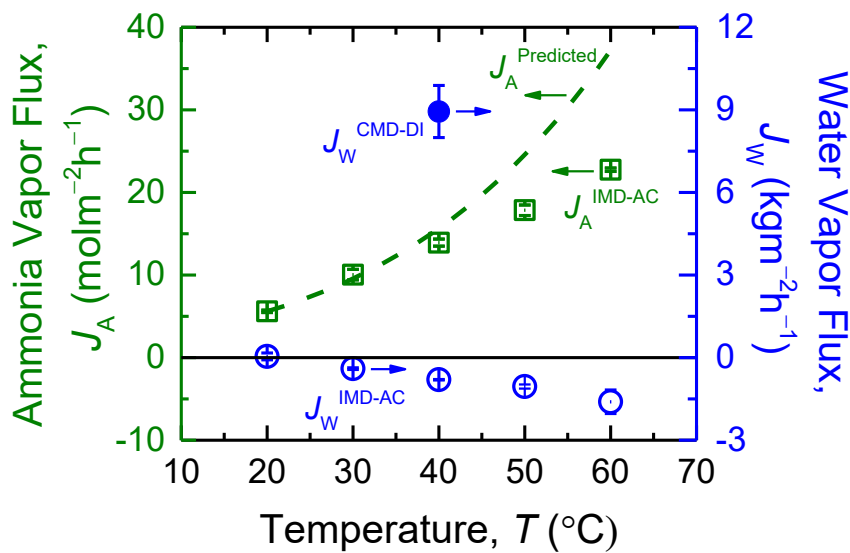
304 Because ammonia present in the DI water collector exhibits vapor pressure, i.e., $P_{C,A} > 0$,
 305 the driving force for NH₃ permeation, $P_{F,A} - P_{C,A}$, is lowered. However, vapor pressure generated
 306 by NH_{3(aq)} in the DI water collector is marginal and, hence, does not fully account for the difference
 307 in J_A between DI water and acidic collector. At the end of the hour-long experiments, ammonia

308 concentration in the collector only reached 8.43 mM and 8.66 mM for CMD-DI and IMD-DI,
309 respectively, equivalent to a reduction in ammonia vapor pressure gradient of 1.5 and 3.8% (drop
310 for isothermal operation is higher because the collector stream is at 40 °C, as opposed to 20 °C for
311 conventional operation). In contrast, the decrease in ammonia vapor fluxes when the collector is
312 DI water instead of acetic acid was 31.6% and 32.0% for CMD and IMD, respectively. Therefore,
313 the slight decline in P_A gradient when TAN is present as $\text{NH}_3\text{(aq)}$ does not adequately explain the
314 considerably smaller J_A with DI water collector.

315 An increase in ammonia vapor flux when acidic solutions were utilized as collector had
316 been reported,^{62,91} but the mechanism was not discussed. We postulate that the J_A enhancement is
317 due to the acidic solution improving the kinetics of ammonia vapor dissolution into the aqueous
318 phase. At the collector side vapor-liquid interface, some ammonia molecules incident on the liquid
319 surface are reflected back into the vapor phase, i.e., condensation coefficient < 1,⁹² resulting in the
320 $\text{NH}_3\text{(g)}$ solubilization rate being slower than the initial rate of ammonia permeation. The molecular
321 reflection builds up the partial vapor pressure of ammonia at the interface and results in $P_{C,A} >$
322 $K_{HCC,A}$, where K_H is Henry's constant for NH_3 .⁹² That is, the vapor-liquid interface at the collector
323 side is not at thermodynamic equilibrium. When a non-acidic solution, such as DI water, is
324 employed for the collector stream, the ammonia solubilization kinetics is slow and the eventual
325 steady-state effective driving force is considerably lessened due to the elevated interfacial $P_{C,A}$.
326 On the other hand, $\text{NH}_3\text{(g)}$ dissolves significantly faster into an acidic solution,⁹³ i.e., condensation
327 coefficient is increased, giving rise to a larger $P_{F,A} - P_{C,A}$ and yielding markedly enhanced ammonia
328 vapor flux. Therefore, the use of AC beneficially improves ammonia separation and recovery by
329 mitigating the kinetic limitation of ammonia dissolution.

330 **Ammonia Vapor Flux Increases with Greater Feed Temperature.** To investigate
331 the influence of temperature on IMD-AC performance, ammonia and water vapor fluxes were
332 characterized as a function of feed and collector solution temperature and presented in Figure 4
333 (green square symbols, left vertical axis and blue circle symbols, right vertical axis, respectively).
334 Ammonia vapor flux monotonically increased from 5.60 to 22.8 $\text{mol m}^{-2}\text{h}^{-1}$ (approximately 4-fold)
335 as operating temperatures were raised from 20 to 60 °C. Critically, the magnitude of water vapor
336 flux was suppressed to below $\approx 2 \text{ kg m}^{-2}\text{h}^{-1}$ across the assessed temperature range, substantially
337 smaller compared to J_w in CMD (blue triangle symbol in Figure 4 for feed and collector solutions
338 at 40 and 20 °C, respectively). As discussed earlier, the direction of water vapor permeation in

339 IMD operation is reversed, i.e., from collector to feed side. This reverse water vapor flux increased
 340 with increasing temperature. This is because ammonia permeation is enhanced at higher
 341 temperatures and, thus, more heat of vaporization was transferred from the feed to collector side,
 342 causing more severe temperature polarization at the solution-membrane interfaces (previously
 343 elaborated and illustrated by Figure S3 of Supporting Information). Hence, the transmembrane
 344 temperature gradient is more pronounced at higher temperatures, resulting in greater reverse water
 345 vapor permeation.



346

347 **Figure 4.** Experimental IMD-AC ammonia and water vapor fluxes (green square symbols, left vertical
 348 axis and blue circle symbols, right vertical axis, respectively) as a function of operating temperature.
 349 Predicted ammonia vapor flux, calculated using eq 1 with membrane vapor permeability coefficient at
 350 20 °C ($L_A = 0.021 \text{ mol m}^{-2} \text{ h}^{-1} \text{ Pa}^{-1}$), is represented by the green dashed line. For comparison, the water
 351 vapor flux in IMD-DI with feed and collector solutions at 40 and 20 °C, respectively, is denoted by the
 352 blue triangle symbol. Error bars indicate standard deviations of duplicate experiments with different
 353 membrane coupon.

354 Low relative vapor flux of water to ammonia for IMD-AC was, again, consistently attained
 355 across the temperatures investigated (Figure S6 of Supporting Information). Magnitude of relative
 356 flux increased slightly with higher temperatures, but was maintained below $-0.1 \text{ kg-H}_2\text{O/mol-NH}_3$
 357 (marginally positive J_W/J_A at 20 °C is attributed to inherent experimental uncertainties in
 358 measuring very small water fluxes). Crucially, ammonia permeation was obtained with adequate
 359 NH₃-H₂O flux selectivity even at the lowest investigated temperature of 20 °C, which is effectively
 360 ambient condition. Hence, the separation and recovery of ammonia from hydrolyzed urine can

361 potentially be achieved, albeit at slower rates, without heating the feed and collector streams to
362 elevate the temperatures.

363 With negligible $\text{NH}_3\text{(aq)}$ concentration in the collector stream, the higher vapor pressure of
364 ammonia at the feed side due to the greater solution temperature results in an augmented driving
365 force for $\text{NH}_3\text{(g)}$ permeation. However, J_A enhancements with increasing temperature is poorly
366 predicted by the governing flux equation, eq 1, and the Clausius-Clapeyron relation. Using the
367 ammonia vapor pressure gradient at each temperature and membrane vapor permeability
368 coefficient at 20 °C ($L_A = 0.022 \text{ mol m}^{-2} \text{ h}^{-1} \text{ Pa}^{-1}$), ammonia vapor fluxes were computed and shown
369 in Figure 4 as the green dashed line. Theoretical calculations overestimate the experimental
370 ammonia vapor fluxes, with greater deviations observed at higher temperatures. Theory forecast
371 an exponential increase in J_A with rising temperature, due to the exponential dependence of vapor
372 pressure on temperature, but an effectively linear increase in experimental ammonia vapor flux
373 was seen.

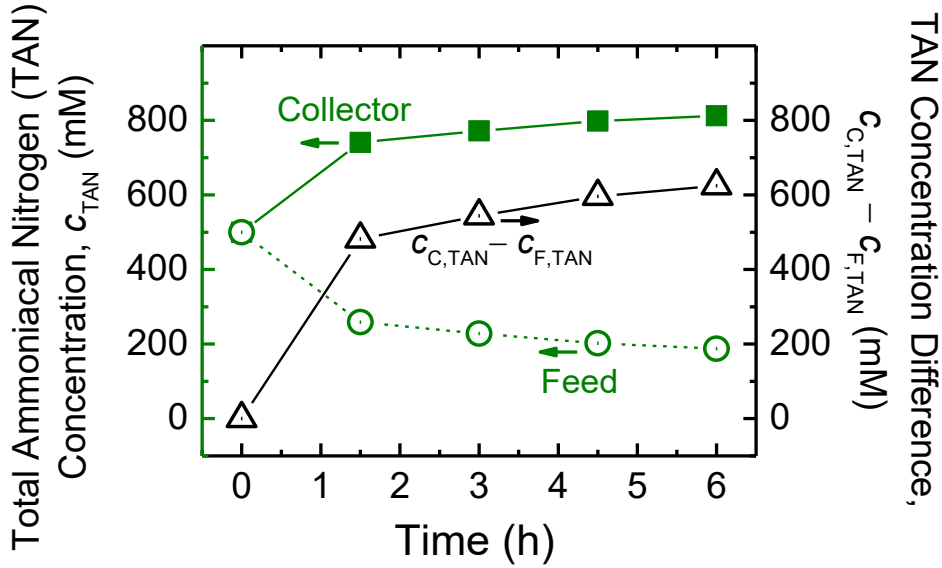
374 One potential explanation for the experimental deviation from expected trend is kinetic
375 limitations for ammonia solubilization into the collector solution (as discussed in the preceding
376 section) being more pronounced at higher temperatures. Alternatively/additionally, NH_3
377 volatilization from the feed solution can be a rate-limiting factor. In the earlier section, we
378 discussed that the liquid and vapor phases at the solution-membrane interfaces are not in
379 equilibrium because ammonia vapor transport across the membrane pores is faster than NH_3
380 volatilizing from the feed stream and/or dissolving into the collector stream.^{92,94,95} Therefore the
381 effective vapor pressures of ammonia at the feed and collector interfaces are lower and higher,
382 respectively, than the equilibrium P_A as governed by Henry's law, i.e., $P_{F,A} < K_{HCF,A}$ and $P_{C,A} >$
383 $K_{HCC,A}$. Given larger ammonia vapor fluxes are obtained at higher IMD operating temperatures,
384 the effect of volatilization and solubilization kinetic limitations is, thus, expected to be more
385 amplified. Consequently, the relative reduction in effective driving force, $P_{F,A} - P_{C,A}$, is greater and
386 actual J_A deviates further from prediction (Figure 4).

387 Another possible cause contributing to the observed disagreement is that water vapor
388 transport in the reverse direction during IMD hinders ammonia permeation. As described by
389 Maxwell-Stefan diffusion, mutual interaction between the NH_3 and H_2O molecules results in
390 frictional drag on the transport of ammonia by water vapor permeating in the opposite direction.⁹⁶

391 ⁹⁸ This resistance to $\text{NH}_3\text{(g)}$ transport scales with the magnitude of reverse $\text{H}_2\text{O(g)}$ flux. Reverse
392 water vapor transport is greater at higher operating temperatures (blue circle symbols of Figure 4)
393 and, hence, the discrepancy between theoretical and experimental fluxes is wider.

394 A third phenomenon that causes experimental fluxes to diverge from calculated J_A is
395 temperature polarization.^{88,89} As discussed earlier, although the bulk solution streams are at the
396 same temperature in IMD, a transmembrane temperature gradient is set up from the collector to
397 feed sides (Figure S3 of Supporting Information), due to the transfer of NH_3
398 volatilization/condensation enthalpy. Interfacial temperature at the feed and collector sides are,
399 hence, lower and higher, respectively, than the bulk solution temperatures. Thus, the effective
400 driving force for ammonia permeation, $P_{\text{F},\text{A}} - P_{\text{C},\text{A}}$, is lesser than the calculated value using bulk
401 solution temperatures. The observed reverse water vapor flux is greater at higher temperatures,
402 indicating that the transmembrane temperature gradient is steeper, i.e., temperature polarization is
403 more acute. Therefore, the deviation between experimental and predicted J_A is anticipated to be
404 larger with increasing temperatures. This mechanism is supported by previous studies that reported
405 decreased apparent membrane vapor transport coefficient with higher temperatures, (i.e.,
406 temperature polarization effects incorporated into L).^{54,56}

407 **High Ammonia Recovery can be Achieved using IMD-AC.** To investigate the
408 potential ammonia recovery yield achievable with IMD-AC from source-separated urine, a batch
409 experiment was conducted with closed-loop recirculation of the solutions across the bench-scale
410 membrane cell, which equivalently simulates co-current flow configuration in a process-scale
411 membrane module. Feed stream TAN (= $\text{NH}_3 + \text{NH}_4^+$) concentration is 500 mM to represent
412 hydrolyzed urine, whereas collector stream is 750 mM acetic acid (higher concentration was
413 employed to avoid pH increases limiting ammonia transport) and 500 mM TAN, i.e., total
414 ammoniacal nitrogen is equal on both sides. TAN concentration of the feed and collector streams
415 in IMD-AC at 40 °C as a function of time is presented in Figure 5 (green circle and square symbols,
416 respectively).



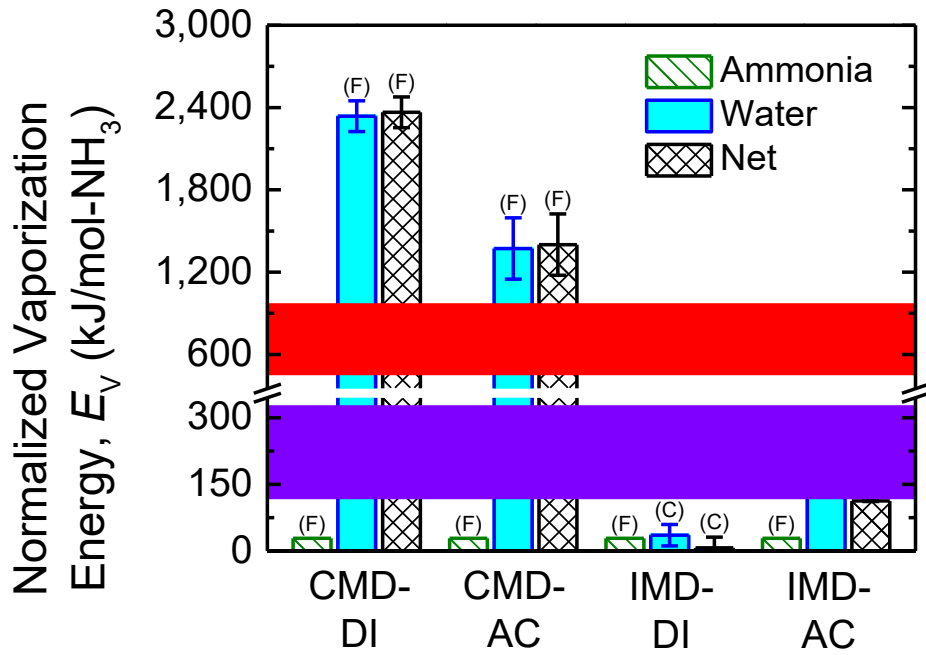
417

418 **Figure 5.** Total ammoniacal nitrogen, TAN, concentration in the feed and collector streams in IMD-AC
 419 operation at 40 °C as a function of time (left vertical axis, green circle and square symbols, respectively).
 420 Feed stream has 500 mM TAN to simulate hydrolyzed urine and collector solution is 500 mM TAN and
 421 750 mM acetic acid (i.e., same initial TAN concentrations for both feed and collector solutions). The
 422 black triangle symbols (right vertical axis) represent the difference between the concentration of TAN
 423 in the collector and feed streams, i.e., $c_{C,TAN} - c_{F,TAN}$.

424 After 1.5 h, collector TAN concentration increased to 741 mM while $c_{F,TAN}$ dropped to 259
 425 mM, representing NH₃ separation and recovery of 48.2%. Comparatively, TAN recovery in IMD
 426 at 40 °C with a DI water collector stream was only 2.7% for the same time period (projected using
 427 J_A of the first 60 min). At the end of 6 h, ≈60% of TAN in the simulated urine was removed and
 428 captured in the collector stream, demonstrating the potential for high ammonia recovery using
 429 IMD-AC. Water flux was practically negligible and solution volumes are effectively unchanged
 430 (< 1% difference after 6 h). As ammonia permeates from the feed to collector side, TAN
 431 concentration and, correspondingly, volatile NH_{3(aq)} concentration of the feed solution decreases.
 432 Consequently, ammonia vapor pressure, $P_{F,A}$, falls and the driving force for ammonia permeation,
 433 $P_{F,A} - P_{C,A}$, declines over time, which is evident by the diminishing rate of change of TAN. Final
 434 pH of the collector solution is 3.5. Given the pK_a of ammonia at 40 °C is 8.8, effectively 100% of
 435 TAN in the bulk collector solution was present as nonvolatile ammonium, NH₄⁺. Hence, NH_{3(aq)}
 436 concentration was negligible, i.e., $c_{C,A} \approx 0$, and ammonia vapor pressure in the collector, $P_{C,A}$, is
 437 practically zero.

438 Crucially, the difference in TAN between the collector and feed solutions, $c_{C,TAN} - c_{F,TAN}$,
439 increased from 0 to ≈ 600 mM (black triangle symbols of Figure 5), indicating transport of
440 ammoniacal nitrogen up a concentration gradient. The “uphill” transport of TAN shows IMD-AC
441 can concentrate ammoniacal nitrogen significantly above the initial $c_{F,TAN}$. In actual module-scale
442 operation, the feed and collector streams will be circulated in counter-current flow and higher
443 recovery yields of ammonia can be achieved with lower acid concentrations in the collector
444 solution.

445 **Substantial Energy Saving is Obtained with IMD.** In membrane distillation, thermal
446 energy is required for the vaporization enthalpy of volatile components that permeate across the
447 membrane.^{55,90,99} Convective heat flux of component i is the product of the vaporization enthalpy,
448 ΔH_i , and the flux, J_i .⁵⁵ Figure 6 shows the vaporization energy for ammonia and water (green
449 patterned and blue solid columns, respectively) in the four operating modes. To exclude the
450 influence of different kinetics (i.e., different $\text{NH}_3(\text{g})$ fluxes), $\Delta H_i J_i$ is divided by J_A to yield energy
451 per mole of ammonia recovered, $E_{V,i}$. Sum of the ammonia and water components gives the net
452 normalized vaporization energy (black patterned columns),
453 $|\sum E_{V,i}| = |J_A^{-1} \sum \Delta H_i J_i| = |\Delta H_A + \Delta H_W J_W / J_A|$ (note that J_i can be negative and the impact on energy
454 required is discussed later). Determination of enthalpy of ammonia vaporization from an aqueous
455 solution, as opposed to a pure liquid, is presented in the Supporting Information, and ΔH_i at the
456 relevant stream temperatures were used in the analysis.^{100,101}



457

458 **Figure 6.** Vaporization energy for ammonia and water (green patterned and blue solid columns, respectively)
459 per mole of ammonia separated and recovered in CMD-DI, CMD-AC, IMD-DI, and IMD-AC. Labels (F) and
460 (C) above the columns denote heat supply to feed and collector streams, respectively. Patterned black columns
461 represent the net vaporization energies of ammonia and water, i.e., $|\sum E_{V,(F)} - \sum E_{V,(C)}|$. Error bars for
462 vaporization of water are standard deviations of duplicate water vapor flux measurements. For comparison, the
463 red- and violet-shaded regions indicate energy required by the Haber-Bosch process, 448-973 kJ/mol-NH₃ (8.89-
464 19.3 kWh/kg-N), and nitrification-denitrification, 116-328 kJ/mol-NH₃ (2.3-6.5 kWh/kg-N), respectively.

465 Whereas normalized energy demand for the vaporization of ammonia, $E_{V,A}$, in the four
466 different operating conditions are the same at 28.4 kJ/mol-NH₃ (due to normalization by J_A), the
467 heat to vaporize water, $E_{V,W}$, varies markedly because it is dependent on the relative vapor flux of
468 water to ammonia (Figure 3). In the conventional MD operations of CMD-DI and CMD-AC,
469 considerable thermal energy of 2,340 and 1,370 kJ/mol-NH₃ (46.4 and 27.2 kWh/kg-N),
470 respectively, is required to evaporate water from the feed solution, 82.4 and 48.2× the energy to
471 volatilize ammonia. The high heat input is because of the large magnitude of inevitable water vapor
472 flux in conventional MD. In contrast, due to suppression of water transport in isothermal MD, $E_{V,W}$
473 is substantially lessened to 35.4 and 141 kJ/mol-NH₃ (0.702 and 2.80 kWh/kg-N) for IMD-DI and
474 IMD-AC, respectively. Since direction of J_W is from the collector to feed side in IMD, i.e., reversed,
475 heat is required for water vaporization at the collector stream (instead of feed side) and is indicated

476 by the label (C). Thermal energy for enthalpy of vaporization is transferred to the other side as
477 enthalpy of condensation when the vapor permeates across the membrane and solubilizes into the
478 aqueous stream. Therefore, the net normalized energy input is the difference between E_v on the
479 feed and collector sides (black patterned columns). Compared to CMD-DI, IMD-AC requires 95.2%
480 less heat input for vaporization to separate and recover the same amount of ammonia by inhibiting
481 undesired water flux (Figure 2). Higher energy savings of 99.7% is achievable with IMD-DI, but
482 NH_3 recovery yield would be constrained (as discussed in preceding section).

483 In addition to convective heat flux discussed above, conduction of heat through the
484 membrane is another thermal energy requirement.^{99,102,103} Conductive heat flux is proportional to
485 the transmembrane temperature differential. Conventional MD necessitates a temperature
486 difference between the feed and collector solutions, whereas the bulk stream temperatures are
487 equal in isothermal MD. Therefore, the temperature gradient across the membrane in IMD is
488 significantly smaller than CMD (Figures 1 and S3) and consequently, conductive heat loss is
489 expected to be minimized in isothermal operation. Moreover, transmembrane heat conduction
490 drives the feed and collector solutions toward temperature equilibrium, which is the working
491 principle of isothermal MD but is against the operation of conventional MD.

492 Overall, isothermal MD favorably reduces the energy consumption for ammonia removal
493 and reuse by substantially lowering both convective and conductive heat input. Compared to
494 energy demand for the current linear economy management of nitrogen, i.e., production by the
495 Haber-Bosch process and removal by conventional nitrification-denitrification, the vaporization
496 energy required for NH_3 recovery in IMD is significantly lower. Energy demand for N fixation by
497 the Haber-Bosch process, the principal ammonia production method, is 8.9-19.3 kWh/kg-N (448-
498 973 kJ/mol- NH_3 , indicated by the red-shaded region in Figure 6). Conventional removal of
499 nitrogen by nitrification and denitrification at wastewater treatment plants demands 2.3-6.5
500 kWh/kg-N (116-328 kJ/mol- NH_3 , indicated by the violet-shaded region). Vaporization energy
501 needed for isothermal MD is around an order of magnitude lower than the Haber-Bosch energy
502 consumption benchmark and is in the same range as nitrification-denitrification. Actual energy
503 requirement for a practical IMD-AC system to remove and recover ammonia from diverted urine
504 will have to factor in auxiliary components (e.g., pumping cost, conductive losses, and heat
505 exchanger efficiency) and module-scale effects, but the first-order energy analysis conducted here

506 highlights potential of the technology to be a competitive alternative to current NH₃ production
507 and removal methods.

508 **IMPLICATIONS**

509 Removal of ammonia from wastewaters is imperative for environmental, ecological, and public
510 health protection. At the same time, nitrogen is a principal component of fertilizer. The high
511 ammonia content in urine offers attractive opportunities to simultaneously recover the resource
512 and remove the contaminant from the waste stream. To align with the principles of green
513 engineering and realize viable implementation, the ammonia separation and recovery approach
514 needs to be energy-efficient.³⁶ This study demonstrates isothermal membrane distillation with
515 acidic collector can achieve i) selective removal and capture of ammonia from hydrolyzed urine
516 with ii) low thermal energy requirements and iii) high recovery yield.

517 Importantly, because only mild temperatures are needed to drive the process, isothermal
518 MD can utilize low-grade heat from locally-available waste flows (e.g., warm bathwater runoff or
519 hot stream of cooling water systems) or onsite low-concentration solar thermal collectors,¹⁰⁴⁻¹⁰⁶
520 further enhancing sustainability of the technology. The study also showed that ammonia separation
521 and recovery is possible even at ambient temperatures, i.e., without further warming up the feed
522 and collector streams, at the expense of lower fluxes. Acid for the collector solution can be from
523 unwanted effluent streams, such as spent pickling brine, which is effectively vinegar (i.e., acetic
524 acid), from the food industry.^{107,108} This study examined the use of acetic acid, but other suitable
525 acids from waste/low-cost sources can be employed. Additionally, IMD-AC can drive the uphill
526 transport of ammoniacal nitrogen to achieve highly concentrated NH₃ solutions as product,
527 favorably minimizing the liquid volume for handling and transport. Crucially, vaporization energy
528 requirement for isothermal MD is substantially below the energy demand for fossil fuel-driven
529 Haber-Bosch process, the dominant ammonia production method, and comparable to energy
530 consumption for N removal at conventional WWTPs. Further techno-economic assessments are
531 needed to quantify the capital and operating expenditure of IMD-AC, but the technology shows
532 initial promise to be a cost-competitive and environmentally-sensible technique for removing and
533 recovering ammonia from source-separated urine.

534 With the projected urban influx of 2.5 billion people by 2050,¹⁰⁹ the population density of
535 cities is expected to increase dramatically. At the same time, providing improved sanitation to the
536 2.3 billion people globally who are currently unserved will necessitate the installation of new
537 toilets, wastewater facilities, and sanitation infrastructure.¹¹⁰ These population and sanitation
538 trends present ideal opportunities for the introduction of decentralized urine diversion facilities for
539 nutrient recovery, without costly retrofits or overhauls of the existing system, shifting wastewater
540 management to a more sustainable and efficient paradigm.

541 Other potential applications of the technology include the selective separation/recovery of
542 compounds that speciate between volatile and nonvolatile forms at different pH. An
543 environmentally-relevant example is H₂S in domestic and industrial wastewaters.¹¹¹ Because of
544 the pH-dependent volatility, H₂S_(g) permeates across the MD membrane and speciates to
545 nonvolatile HS⁻_(aq) in a basic collector (equivalent to NH_{3(g)} transport and speciation to NH₄₊_(aq)),
546 thus, enabling selective removal, capture, and concentration.

547 **ASSOCIATED CONTENT**

548 **Supporting Information**

549 The Supporting Information is available free of charge at
550 <https://pubs.acs.org/doi/10.1021/acssuschemeng.xxx>.

551 Determination of ammonia and water vapor pressures; speciation of total ammoniacal
552 nitrogen (Figure S1); bench-scale membrane distillation setup utilized in experiments
553 (Figure S2); temperature and vapor pressure profiles in membrane distillation (Figure S3);
554 relative vapor flux of water to ammonia in kg-H₂O/mol-NH₃ for each operation (Figure
555 S4); collector solution pH as a function of time under each operation (Figure S5); relative
556 molar flux of water to ammonia in IMD-AC as a function of temperature (Figure S6);
557 determination of the vaporization enthalpy of ammonia from aqueous solutions.

558 **AUTHOR INFORMATION**

559 **Corresponding Author**

560 Ngai Yin Yip — *Department of Earth and Environmental Engineering and Columbia Water*
561 *Center, Columbia University, New York, New York 10027-6623, United States;*
562 orcid.org/0000-0002-1986-4189; Phone: +1 (212) 854-2984; Email:n.y.yip@columbia.edu

563 **Authors**

564 Stephanie N. McCartney — *Department of Earth and Environmental Engineering, Columbia*
565 *University, New York, New York 10027-6623, United States*

566 Natalie A. Williams — *Department of Earth and Environmental Engineering, Columbia*
567 *University, New York, New York 10027-6623, United States*

568 Chanhee Boo — *Department of Earth and Environmental Engineering, Columbia University,*
569 *New York, New York 10027-6623, United States;* orcid.org/0000-0003-4595-9963

570 Xi Chen — *Department of Earth and Environmental Engineering, Columbia University, New*
571 *York, New York 10027-6623, United States*

572 Complete contact information is available at: <https://pubs.acs.org/10.1021/acssuschemeng.xxx>

573 **Notes**

574 The authors declare no competing financial interest.

575 **ACKNOWLEDGEMENT**

576 This material is based upon work supported by the National Science Foundation under Grant No.
577 1903705.

578 **REFERENCES**

579 1. NAE Grand Challenges for Engineering, <https://www.nae.edu/File.aspx?id=187214> (Accessed
580 on 02/20/2019)

581 2. Steffen, W.; Richardson, K.; Rockstrom, J.; Cornell, S. E.; Fetzer, I.; Bennett, E. M.; Biggs, R.;
582 Carpenter, S. R.; de Vries, W.; de Wit, C. A.; Folke, C.; Gerten, D.; Heinke, J.; Mace, G. M.;
583 Persson, L. M.; Ramanathan, V.; Reyers, B.; Sorlin, S., Planetary boundaries: Guiding human
584 development on a changing planet. *Science* **2015**, *347*, (6223). DOI: UNSP 1259855
585 10.1126/science.1259855.

586 3. Michalak, A. M.; Anderson, E. J.; Beletsky, D.; Boland, S.; Bosch, N. S.; Bridgeman, T. B.;
587 Chaffin, J. D.; Cho, K.; Confesor, R.; Daloglu, I.; DePinto, J. V.; Evans, M. A.; Fahnstiel, G. L.;
588 He, L.; Ho, J. C.; Jenkins, L.; Johengen, T. H.; Kuo, K. C.; LaPorte, E.; Liu, X.; McWilliams, M.
589 R.; Moore, M. R.; Posselt, D. J.; Richards, R. P.; Scavia, D.; Steiner, A. L.; Verhamme, E.; Wright,
590 D. M.; Zagorski, M. A., Record-setting algal bloom in Lake Erie caused by agricultural and
591 meteorological trends consistent with expected future conditions. *Proc. Natl. Acad. Sci.* **2013**, *110*,
592 (16), 6448-6452. DOI: 10.1073/pnas.1216006110.

593 4. Conley, D. J.; Paerl, H. W.; Howarth, R. W.; Boesch, D. F.; Seitzinger, S. P.; Havens, K. E.;
594 Lancelot, C.; Likens, G. E., Ecology - Controlling eutrophication: Nitrogen and phosphorus.
595 *Science* **2009**, *323*, 1014-1015. DOI: 10.1126/science.1167755.

596 5. Diaz, R. J.; Rosenberg, R., Spreading dead zones and consequences for marine ecosystems.
597 *Science* **2008**, *321*, 926-929. DOI: 10.1126/science.1156401.

598 6. Brooks, B. W.; Lazorchak, J. M.; Howard, M. D. A.; Johnson, M. V. V.; Morton, S. L.; Perkins,
599 D. A. K.; Reavie, E. D.; Scott, G. I.; Smith, S. A.; Steevens, J. A., Are Harmful Algal Blooms
600 Becoming the Greatest Inland Water Quality Threat to Public Health and Aquatic Ecosystems?
601 *Environ. Toxicol. Chem.* **2016**, *35*, (1), 6-13. DOI: 10.1002/etc.3220.

602 7. Hitzfeld, B. C.; Hoger, S. J.; Dietrich, D. R., Cyanobacterial toxins: Removal during drinking
603 water treatment, and human risk assessment. *Environ. Health Persp.* **2000**, *108*, 113-122. DOI:
604 Doi 10.2307/3454636.

605 8. Environmental Protection Agency. Clean Watersheds Needs Survey In 2012.

606 9. Rahman, S. M.; Eckelman, M. J.; Onnis-Hayden, A.; Gu, A. Z., Life-Cycle Assessment of
607 Advanced Nutrient Removal Technologies for Wastewater Treatment. *Environ. Sci. Technol.* **2016**.
608 DOI: 10.1021/acs.est.5b05070.

609 10. Maurer, M.; Schwegler, P.; Larsen, T. A., Nutrients in urine: energetic aspects of removal and
610 recovery. *Water Sci. Technol.* **2003**, *48*, (1), 37-46. DOI: <https://doi.org/10.2166/wst.2003.0011>

611 11. Mulder, A., The quest for sustainable nitrogen removal technologies. *Water Sci. Technol.* **2003**,
612 *48*, (1), 67-75. DOI: <https://doi.org/10.2166/wst.2003.0018>

613 12. Wett, B., Development and implementation of a robust deammonification process. *Water Sci.*
614 *Technol.* **2007**, *56*, (7), 81-88. DOI: 10.2166/wst.2007.611.

615 13. Schaubroeck, T.; De Clippeleir, H.; Weissenbacher, N.; Dewulf, J.; Boeckx, P.; Vlaeminck, S.
616 E.; Wett, B., Environmental sustainability of an energy self-sufficient sewage treatment plant:
617 Improvements through DEMON and co-digestion. *Water Res.* **2015**, *74*, 166-179. DOI:
618 10.1016/j.watres.2015.02.013.

619 14. Erisman, J. W.; Sutton, M. A.; Galloway, J.; Klimont, Z.; Winiwarter, W., How a century of
620 ammonia synthesis changed the world. *Nat. Geosci.* **2008**, *1*, (10), 636-741. DOI:
621 10.1038/ngeo325.

622 15. Fowler, D.; Coyle, M.; Skiba, U.; Sutton, M. A.; Cape, J. N.; Reis, S.; Sheppard, L. J.; Jenkins,
623 A.; Grizzetti, B.; Galloway, J. N.; Vitousek, P.; Leach, A.; Bouwman, A. F.; Butterbach-Bahl, K.;
624 Dentener, F.; Stevenson, D.; Amann, M.; Voss, M., The global nitrogen cycle in the Twentyfirst
625 century. *Philos. Trans. R. Soc. B* **2013**, *368*, (1621). DOI: 10.1098/rstb.2013.0164.

626 16. Chen, J. G.; Crooks, R. M.; Seefeldt, L. C.; Bren, K. L.; Bullock, R. M.; Daresbourg, M. Y.;
627 Holland, P. L.; Hoffman, B.; Janik, M. J.; Jones, A. K.; Kanatzidis, M. G.; King, P.; Lancaster, K.
628 M.; Lymar, S. V.; Pfromm, P.; Schneider, W. F.; Schrock, R. R., Beyond fossil fuel-driven
629 nitrogen transformations. *Science* **2018**, *360*, (6391). DOI: ARTN eaar6611
630 10.1126/science.aar6611.

631 17. Li, W. W.; Yu, H. Q.; Rittmann, B. E., Chemistry: Reuse water pollutants. *Nature* **2015**, *528*,
632 (7580), 29-31. DOI: 10.1038/528029a.

633 18. Verstraete, W.; de Caveye, P. V.; Diamantis, V., Maximum use of resources present in
634 domestic "used water". *Bioresour. Technol.* **2009**, *100*, (23), 5537-5545. DOI:
635 10.1016/j.biortech.2009.05.047.

636 19. Guest, J. S.; Skerlos, S. J.; Barnard, J. L.; Beck, M. B.; Daigger, G. T.; Hilger, H.; Jackson, S.
637 J.; Karvazy, K.; Kelly, L.; Macpherson, L.; Mihelcic, J. R.; Pramanik, A.; Raskin, L.; Van
638 Loosdrecht, M. C. M.; Yeh, D.; Love, N. G., A new planning and design paradigm to achieve
639 sustainable resource recovery from wastewater. In *Environ. Sci. Technol.*, 2009.

640 20. Epstein, E., *Land Application of Sewage Sludge and Biosolids*. 1 ed.; CRC Press: Boca Raton,
641 **2002**.

642 21. Lu, Q.; He, Z. L.; Stoffella, P. J., Land Application of Biosolids in the USA: A Review. *Appl.*
643 *and Environ. Soil Sci.* **2012**. DOI: 10.1155/2012/201462.

644 22. Gerba, C. P.; Pepper, I. L.; Whitehead, L. F., A risk assessment of emerging pathogens of
645 concern in the land application of biosolids. *Water Sci. Technol.* **2002**, *46*, (10), 225-230. DOI:
646 <https://doi.org/10.2166/wst.2002.0338>

647 23. Brooks, J. P.; Tanner, B. D.; Josephson, K. L.; Gerba, C. P.; Haas, C. N.; Pepper, I. L., A
648 national study on the residential impact of biological aerosols from the land application of
649 biosolids. *J. Appl. Microbiol.* **2005**, *99*, (2), 310-322. DOI: 10.1111/j.1365-2672.2005.02604.x.

650 24. Bright, D. A.; Healey, N., Contaminant risks from biosolids land application: Contemporary
651 organic contaminant levels in digested sewage sludge from five treatment plants in Greater
652 Vancouver, British Columbia. *Environ. Pollut.* **2003**, *126*, (1), 39-49. DOI: 10.1016/S0269-
653 7491(03)00148-9.

654 25. Lapen, D. R.; Topp, E.; Metcalfe, C. D.; Li, H.; Edwards, M.; Gottschall, N.; Bolton, P.; Curnoe,
655 W.; Payne, M.; Beck, A., Pharmaceutical and personal care products in tile drainage following
656 land application of municipal biosolids. *Sci. Total Environ.* **2008**, *399*, (1-3), 50-65. DOI:
657 10.1016/j.scitotenv.2008.02.025.

658 26. Lake, D. L.; Kirk, P. W. W.; Lester, J. N., Fractionation, Characterization, and Speciation of
659 Heavy-Metals in Sewage-Sludge and Sludge-Amended Soils - a Review. *J. Environ. Qual.* **1984**,
660 *13*, (2), 175-183. DOI: DOI 10.2134/jeq1984.00472425001300020001x.

661 27. Yetilmezsoy, K.; Sapci-Zengin, Z., Recovery of ammonium nitrogen from the effluent of
662 UASB treating poultry manure wastewater by MAP precipitation as a slow release fertilizer. *J.*
663 *Hazard. Mater.* **2009**, *166*, (1), 260-269. DOI: 10.1016/j.hazmat.2008.11.025.

664 28. Cai, T.; Park, S. Y.; Li, Y. B., Nutrient recovery from wastewater streams by microalgae: Status
665 and prospects. *Renew. Sust. Energ. Rev.* **2013**, *19*, 360-369. DOI: 10.1016/j.rser.2012.11.030.

666 29. Lin, Y.; Guo, M.; Shah, N.; Stuckey, D. C., Economic and environmental evaluation of
667 nitrogen removal and recovery methods from wastewater. *Bioresour. Technol.* **2016**, *215*, 227-238.
668 DOI: <https://doi.org/10.1016/j.biortech.2016.03.064>.

669 30. Batstone, D. J.; Hülsen, T.; Mehta, C. M.; Keller, J., Platforms for energy and nutrient recovery
670 from domestic wastewater: A review. *Chemosphere* **2015**, *140*, 2-11. DOI:
671 <https://doi.org/10.1016/j.chemosphere.2014.10.021>.

672 31. Bilyk, K.; Bustamante, H.; Connor, M.; deBarbadillo, C.; Downing, L.; Dupont, R.; Fattah, K.;
673 Finch, R.; Gray, D.; Harper, W., Nutrient Recovery: State of the Knowledge. *Water Environ. Res.*
674 *Foundation* **2011**, *1*, 1-19.

675 32. Mehta, C. M.; Khunjar, W. O.; Nguyen, V.; Tait, S.; Batstone, D. J., Technologies to Recover
676 Nutrients from Waste Streams: A Critical Review. *Critical Reviews in Environ. Sci. Technol.* **2015**,
677 *45*, (4), 385-427. DOI: 10.1080/10643389.2013.866621.

678 33. Pastor, L.; Mangin, D.; Ferrer, J.; Seco, A., Struvite formation from the supernatants of an
679 anaerobic digestion pilot plant. *Bioresour. Technol.* **2010**, *101*, (1), 118-125. DOI:
680 10.1016/j.biortech.2009.08.002.

681 34. Desloover, J.; Abate Woldeyohannis, A.; Verstraete, W.; Boon, N.; Rabaey, K.,
682 Electrochemical Resource Recovery from Digestate to Prevent Ammonia Toxicity during
683 Anaerobic Digestion. *Environ. Sci. Technol.* **2012**, *46*, (21), 12209-12216. DOI:
684 10.1021/es3028154.

685 35. Ippersiel, D.; Mondor, M.; Lamarche, F.; Tremblay, F.; Dubreuil, J.; Masse, L., Nitrogen
686 potential recovery and concentration of ammonia from swine manure using electrodialysis coupled
687 with air stripping. *J. Environ. Manage.* **2012**, *95*, S165-S169. DOI:
688 <https://doi.org/10.1016/j.jenvman.2011.05.026>.

689 36. Anastas, P. T., and Zimmerman, J.B., Design through the Twelve Principles of Green
690 Engineering. *Environ. Sci. Technol.* **2003**, *37*, (5), 94A-101A. DOI:
691 <https://doi.org/10.1021/es032373g>

692 37. Karak, T.; Bhattacharyya, P., Human urine as a source of alternative natural fertilizer in
693 agriculture: A flight of fancy or an achievable reality. *Resour. Conserv. Recycl.* **2011**, *55*, (4), 400-
694 408. DOI: 10.1016/j.resconrec.2010.12.008.

695 38. Larsen, T. A.; Alder, A. C.; Eggen, R. I. L.; Maurer, M.; Lienert, J., Source separation: Will
696 we see a paradigm shift in wastewater handling? *Environ. Sci. Technol.* **2009**, *43*, (16), 6121. DOI:
697 10.1021/es803001r.

698 39. Simha, P.; Ganesapillai, M., Ecological Sanitation and nutrient recovery from human urine:
699 How far have we come? A review. *Sustain. Environ. Res.* **2017**, *27*, (3), 107-116. DOI:
700 10.1016/j.serj.2016.12.001.

701 40. Gao, X. S., T.; Zheng, Y.; Sun, X.; Huang, S.; Ren, Q.; Zhang, X.; Tian, Y.; Luan, G, *Practical*
702 *manure handbook. In Chinese.* Agricultural Publishing House: Beijing, **2002**.

703 41. Larsen, T. A. U., K. M.; Lienert, J., *Source separation and decentralization for wastewater*
704 *management.* Iwa Publishing: **2013**.

705 42. Jönsson, H. V., B., *Adapting the nutrient content of urine and faeces in different countries*
706 *using FAO and Swedish data,* Proceedings of the 2nd International Symposium on ecological
707 sanitation, **2003**; pp 7-11.

708 43. Mihelcic, J. R.; Fry, L. M.; Shaw, R., Global potential of phosphorus recovery from human
709 urine and feces. *Chemosphere* **2011**, *84*, (6), 832-839. DOI: 10.1016/j.chemosphere.2011.02.046.

710 44. Larsen, T. A.; Hoffmann, S.; Lüthi, C.; Truffer, B.; Maurer, M., Emerging solutions to the
711 water challenges of an urbanizing world. *Science* **2016**, *352*, (6288), 928-933. DOI:
712 10.1126/science.aad8641.

713 45. Randall, D. G.; Naidoo, V., Urine: The liquid gold of wastewater. *J. Environ. Chem. Eng.* **2018**,
714 6, (2), 2627-2635. DOI: 10.1016/j.jece.2018.04.012.

715 46. Maurer, M.; Pronk, W.; Larsen, T. A., Treatment processes for source-separated urine. *Water*
716 *Res.* **2006**, *40*, (17), 3151-3166. DOI: 10.1016/j.watres.2006.07.012. DOI:
717 10.1016/j.watres.2006.07.012.

718 47. Başakçılardan-Kabakci, S.; İpekoğlu, A. N.; Talinli, I., Recovery of Ammonia from Human
719 Urine by Stripping and Absorption. *Environ. Eng. Sci.* **2007**, *24*, (5), 615-624. DOI:
720 10.1089/ees.2006.0412.

721 48. Kabdaşlı, I.; Tunay, O.; İşlek, Ç.; Erdinç, E.; Hüskalar, S.; Tatlı, M. B., Nitrogen recovery by
722 urea hydrolysis and struvite precipitation from anthropogenic urine. *Water Sci. Technol.* **2006**, *53*,
723 (12), 305-312. DOI: 10.2166/wst.2006.433.

724 49. Ledezma, P.; Kuntke, P.; Buisman, C. J. N.; Keller, J.; Freguia, S., Source-separated urine
725 opens golden opportunities for microbial electrochemical technologies. *Trends Biotechnol.* **2015**,
726 33, (4), 214-220. DOI: <https://doi.org/10.1016/j.tibtech.2015.01.007>.

727 50. Udert, K. M.; Wächter, M., Complete nutrient recovery from source-separated urine by
728 nitrification and distillation. *Water Res.* **2012**, *46*, (2), 453-464. DOI:
729 <https://doi.org/10.1016/j.watres.2011.11.020>.

730 51. Kabdaşlı, I.; Tünay, O., Nutrient recovery by struvite precipitation, ion exchange and
731 adsorption from source-separated human urine – a review. *Environ. Technol. Rev.* **2018**, 7, (1),
732 106-138. DOI: 10.1080/21622515.2018.1473504.

733 52. Udert, K. M.; Larsen, T. A.; Biebow, M.; Gujer, W., Urea hydrolysis and precipitation
734 dynamics in a urine-collecting system. *Water Res.* **2003**, 37, (11), 2571-2582. DOI:
735 10.1016/S0043-1354(03)00065-4.

736 53. Liu, Y.; Kumar, S.; Kwag, J. H.; Ra, C., Magnesium ammonium phosphate formation, recovery
737 and its application as valuable resources: a review. *J. Chem. Technol. Biotechnol.* **2013**, 88, (2),
738 181-189. DOI: 10.1002/jctb.3936.

739 54. Lawson, K. W.; Lloyd, D. R., Membrane Distillation *J. Membr. Sci.* **1997**, 124, (1), 1-25. DOI:
740 [https://doi.org/10.1016/S0376-7388\(96\)00236-0](https://doi.org/10.1016/S0376-7388(96)00236-0)

741 55. Alkhudhiri, A.; Darwish, N.; Hilal, N., Membrane distillation: A comprehensive review.
742 *Desalination* **2012**, 287, 2-18. DOI: 10.1016/j.desal.2011.08.027.

743 56. Drioli, E.; Ali, A.; Macedonio, F., Membrane distillation: Recent developments and
744 perspectives. *Desalination* **2015**, 356, 56-86. DOI: 10.1016/j.desal.2014.10.028.

745 57. Zarebska, A.; Nieto, D. R.; Christensen, K. V.; Nordahl, B., Ammonia recovery from
746 agricultural wastes by membrane distillation: Fouling characterization and mechanism. *Water Res.*
747 **2014**, 56, 1-10. DOI: 10.1016/j.watres.2014.02.037.

748 58. Qu, D.; Sun, D.; Wang, H.; Yun, Y., Experimental study of ammonia removal from water by
749 modified direct contact membrane distillation. *Desalination* **2013**, 326, 135-140. DOI:
750 10.1016/j.desal.2013.07.021.

751 59. Duong, T.; Xie, Z.; Ng, D.; Hoang, M., Ammonia removal from aqueous solution by membrane
752 distillation. *Water Environ. J.* **2013**, 27, (3), 425-434. DOI: 10.1111/j.1747-6593.2012.00364.x.

753 60. Bodell, B. R., Distillation of Saline Water Using Silicone Rubber Membrane. U.S. Patent
754 3,361,645A, **1968**.

755 61. Ahn, Y. T.; Hwang, Y. H.; Shin, H. S., Application of PTFE membrane for ammonia removal
756 in a membrane contactor. *Water Sci. Technol.* **2011**, 63, (12), 2944-2948. DOI:
757 10.2166/wst.2011.141.

758 62. Ding, Z.; Liu, L.; Li, Z.; Ma, R.; Yang, Z., Experimental study of ammonia removal from water
759 by membrane distillation (MD): The comparison of three configurations. *J. Membr. Sci.* **2006**, 286,
760 (1-2), 93-103. DOI: 10.1016/j.memsci.2006.09.015.

761 63. Kartohardjono, S.; Fermi, M. I.; Yuliusman; Elkardiana, K.; Sangaji, A. P.; Ramadhan, A. M.,
762 The Removal of Dissolved Ammonia from Wastewater through a Polypropylene Hollow Fiber
763 Membrane Contactor. *Int. J. Technol.* **2015**, 6, (7), 1146-1152. DOI:
764 <https://doi.org/10.14716/ijtech.v6i7.1845>

765 64. Lauterbock, B.; Moder, K.; Germ, T.; Fuchs, W., Impact of characteristic membrane
766 parameters on the transfer rate of ammonia in membrane contactor application. *Sep. Purif. Technol.*
767 **2013**, *116*, 327-334. DOI: 10.1016/j.seppur.2013.06.010.

768 65. Lin, P. H.; Horng, R. Y.; Hsu, S. F.; Chen, S. S.; Ho, C. H., A Feasibility Study of Ammonia
769 Recovery from Coking Wastewater by Coupled Operation of a Membrane Contactor and
770 Membrane Distillation. *Int. J. Environ. Res. Public Health* **2018**, *15*, (3). DOI: ARTN 441
771 10.3390/ijerph15030441.

772 66. Liu, H. Y.; Wang, J. L., Separation of ammonia from radioactive wastewater by hydrophobic
773 membrane contactor. *Prog. Nucl. Energ.* **2016**, *86*, 97-102. DOI: 10.1016/j.pnucene.2015.10.011.

774 67. Lu, J.; Li, B. A.; Wang, L.; Wang, Y.; Wang, S. C., Utilization of ammonia-containing
775 wastewater by combining membrane absorption and vacuum membrane distillation. *J. Chem.*
776 *Technol. Biotechnol.* **2014**, *89*, (2), 312-321. DOI: 10.1002/jctb.4126.

777 68. Tun, L. L.; Jeong, D.; Jeong, S.; Cho, K.; Lee, S.; Bae, H., Dewatering of source-separated
778 human urine for nitrogen recovery by membrane distillation. *J. Membr. Sci.* **2016**, *512*, 13-20.
779 DOI: 10.1016/j.memsci.2016.04.004.

780 69. Xia, Q.; Yun, Y. B.; Chen, J. J.; Qu, D.; Li, C. L.; Zhu, S. W., Treatment of ammonia nitrogen
781 wastewater by membrane distillation using PVDF membranes. *Desalin. Water Treat.* **2017**, *61*,
782 126-135. DOI: 10.5004/dwt.2016.0131.

783 70. Xu, K. N.; Qu, D.; Zheng, M.; Guo, X. H.; Wang, C. W., Water Reduction and Nutrient
784 Reconcentration of Hydrolyzed Urine via Direct-Contact Membrane Distillation: Ammonia Loss
785 and Its Control. *J. Environ. Eng.* **2019**, *145*, (3). DOI: Artn 04018144
786 10.1061/(Asce)Ee.1943-7870.0001496.

787 71. Daguerre-Martini, S.; Vanotti, M. B.; Rodriguez-Pastor, M.; Rosal, A.; Moral, R., Nitrogen
788 recovery from wastewater using gas-permeable membranes: Impact of inorganic carbon content
789 and natural organic matter. *Water Res.* **2018**, *137*, 201-210. DOI:
790 <https://doi.org/10.1016/j.watres.2018.03.013>.

791 72. Vanotti, M. B.; Dube, P. J.; Szogi, A. A.; García-González, M. C., Recovery of ammonia and
792 phosphate minerals from swine wastewater using gas-permeable membranes. *Water Res.* **2017**,
793 *112*, 137-146. DOI: <https://doi.org/10.1016/j.watres.2017.01.045>.

794 73. Kuntke, P.; Zamora, P.; Saakes, M.; Buisman, C. J. N.; Hamelers, H. V. M., Gas-permeable
795 hydrophobic tubular membranes for ammonia recovery in bio-electrochemical systems. *Environ.*
796 *Sci. Water Res. Technol.* **2016**, *2*, (2), 261-265. DOI: 10.1039/C5EW00299K.

797 74. Tarpeh, W. A.; Barazesh, J. M.; Cath, T. Y.; Nelson, K. L., Electrochemical Stripping to
798 Recover Nitrogen from Source-Separated Urine. *Environ. Sci. Technol.* **2018**, *52*, (3), 1453-1460.
799 DOI: 10.1021/acs.est.7b05488.

800 75. EL-Bourawi, M. S.; Khayet, M.; Ma, R.; Ding, Z.; Li, Z.; Zhang, X., Application of vacuum
801 membrane distillation for ammonia removal. *J. Membr. Sci.* **2007**, *301*, (1-2), 200-209. DOI:
802 10.1016/j.memsci.2007.06.021.

803 76. He, Q. Y.; Tu, T.; Yan, S. P.; Yang, X.; Duke, M.; Zhang, Y. L.; Zhao, S. F., Relating water
804 vapor transfer to ammonia recovery from biogas slurry by vacuum membrane distillation. *Sep.*
805 *Purif. Technol.* **2018**, *191*, 182-191. DOI: 10.1016/j.seppur.2017.09.030.

806 77. Sarbatly, R.; Chiam, C. K., Ammonia Removal from Saline Water by Direct Contact
807 Membrane Distillation. In *Sustainable Membrane Technology for Energy, Water, and*
808 *Environment*, Wiley: **2012**; pp 309-317.

809 78. Wu, C. R.; Yan, H. H.; Li, Z. G.; Lu, X. L., Ammonia recovery from high concentration
810 wastewater of soda ash industry with membrane distillation process. *Desalin. Water Treat.* **2016**,
811 *57*, (15), 6792-6800. DOI: 10.1080/19443994.2015.1010233.

812 79. Xie, Z. L.; Duong, T.; Hoang, M.; Nguyen, C.; Bolto, B., Ammonia removal by sweep gas
813 membrane distillation. *Water Res.* **2009**, *43*, (6), 1693-1699. DOI: 10.1016/j.watres.2008.12.052.

814 80. Liu, Q. L.; Liu, C. H.; Zhao, L.; Ma, W. C.; Liu, H. L.; Ma, J., Integrated forward osmosis-
815 membrane distillation process for human urine treatment. *Water Res.* **2016**, *91*, 45-54. DOI:
816 10.1016/j.watres.2015.12.045.

817 81. Rittner, D., Bailey, R.A., Clausius-Clapeyron equation. In *Facts on File science encyclopedia: Encyclopedias of chemistry* (2nd ed.). **2016**.

819 82. Wang, P.; Chung, T. S., Recent advances in membrane distillation processes: Membrane
820 development, configuration design and application exploring. *J. Membr. Sci.* **2015**, *474*, 39-56.
821 DOI: 10.1016/j.memsci.2014.09.016.

822 83. Rezakazemi, M.; Shirazian, S.; Ashrafizadeh, S. N., Simulation of ammonia removal from
823 industrial wastewater streams by means of a hollow-fiber membrane contactor. *Desalination* **2012**,
824 *285*, 383-392. DOI: 10.1016/j.desal.2011.10.030.

825 84. El-Bourawi, M. S.; Ding, Z.; Ma, R.; Khayet, M., A framework for better understanding
826 membrane distillation separation process. *J. Membr. Sci.* **2006**, *285*, (1-2), 4-29. DOI:
827 10.1016/j.memsci.2006.08.002.

828 85. J.M. Smith, H. C. V. N., M. M. Abbott, *Introduction to Chemical Engineering Thermodynamics*. **2005**, 357-358.

830 86. Bates, R. G.; Pinching, G. D., Acidic dissociation constant of ammonium ion at 0 to 50 C, and
831 the base strength of ammonia. *J. Res. Natl. Bur. Stand.* **2012**, *42*, (5), 419-430. DOI:
832 10.6028/jres.042.037.

833 87. Bolleter, W. T.; Bushman, C. J.; Tidwell, P. W., Spectrophotometric Determination of
834 Ammonia as Indophenol. *Anal. Chem.* **1961**, *33*, (4), 592-594. DOI: 10.1021/ac60172a034.

835 88. Schofield, R. W.; Fane, A. G.; Fell, C. J. D., Heat and mass transfer in membrane distillation.
836 *J. Membr. Sci.* **1987**, *33*, (3), 299-313. DOI: 10.1016/S0376-7388(00)80287-2.

837 89. Fane, A. G.; Schofield, R. W.; Fell, C. J. D., The efficient use of energy in membrane
838 distillation. *Desalination* **1987**, *64*, 231-243. DOI: 10.1016/0011-9164(87)90099-3.

839 90. Khayet, M., Membranes and theoretical modeling of membrane distillation: A review. *Adv.*
840 *Colloid Interface Sci.* **2011**, *164*, (1-2), 56-88. DOI: 10.1016/j.cis.2010.09.005.

841 91. Zhu, Z.; Hao, Z.; Shen, Z.; Chen, J., Modified modeling of the effect of pH and viscosity on
842 the mass transfer in hydrophobic hollow fiber membrane contactors. *J. Membr. Sci.* **2005**, *250*, (1-
843 2), 269-276. DOI: 10.1016/j.memsci.2004.10.031.

844 92. Deshmukh, A.; Lee, J., Membrane desalination performance governed by molecular reflection
845 at the liquid-vapor interface. *Int. J. Heat Mass Transf.* **2019**, *140*, 1006-1022. DOI:
846 10.1016/j.ijheatmasstransfer.2019.06.044.

847 93. Shi, Q.; Davidovits, P.; Jayne, J. T.; Worsnop, D. R.; Kolb, C. E., Uptake of gas-phase
848 ammonia. 1. Uptake by aqueous surfaces as a function of pH. *J. Phys. Chem. A.* **1999**, *103*, (44),
849 8812-8823. DOI 10.1021/jp991696p.

850 94. Eames, I. W.; Marr, N. J.; Sabir, H., The evaporation coefficient of water: A review. *Int. J.*
851 *Heat Mass Transf.* **1997**, *40*, (12), 2963-2973. DOI: 10.1016/S0017-9310(96)00339-0.

852 95. Marek, R.; Straub, J., Analysis of the evaporation coefficient and the condensation coefficient
853 of water. *Int. J. Heat Mass Transf.* **2001**, *44*, (1), 39-53. DOI: 10.1016/S0017-9310(00)00086-7.

854 96. Kerkhof, P. J. A. M., A modified Maxwell-Stefan model for transport through inert membranes:
855 The binary friction model. *Chem. Eng. J.* **1996**, *64*, (3), 319-343. DOI: Doi 10.1016/S0923-
856 0467(96)03134-X.

857 97. Krishna, R.; Wesselingh, J. A., Review article number 50 - The Maxwell-Stefan approach to
858 mass transfer. *Chem. Eng. Sci.* **1997**, *52*, (6), 861-911. DOI: Doi 10.1016/S0009-2509(96)00458-
859 7.

860 98. Cussler, E., Multicomponent Diffusion. In *Multicomponent Diffusion*, Elsevier: 2013; p 39.

861 99. Lin, S.; Yip, N. Y.; Elimelech, M., Direct contact membrane distillation with heat recovery:
862 Thermodynamic insights from module scale modeling. *J. Membr. Sci.* **2014**, *453*, 498-515. DOI:
863 10.1016/j.memsci.2013.11.016.

864 100. NIST Chemistry Webook, SRD 69: Ammonia.
865 <https://webbook.nist.gov/cgi/cbook.cgi?ID=7664-41-7> (Accessed on 02/20/2019)

866 101. NIST Chemistry Webook, SRD 69: Water.
867 <https://webbook.nist.gov/cgi/cbook.cgi?ID=C7732185> (Accessed on 02/20/2019)

868 102. Vanneste, J.; Bush, J. A.; Hickenbottom, K. L.; Marks, C. A.; Jassby, D.; Turchi, C. S.; Cath,
869 T. Y., Novel thermal efficiency-based model for determination of thermal conductivity of
870 membrane distillation membranes. *J. Membr. Sci.* **2018**, *548*, 298-308. DOI:
871 10.1016/j.memsci.2017.11.028.

872 103. Leitch, M. E.; Lowry, G. V.; Mauter, M. S., Characterizing convective heat transfer
873 coefficients in membrane distillation cassettes. *J. Membr. Sci.* **2017**, *538*, 108-121. DOI:
874 10.1016/j.memsci.2017.05.028.

875 104. Kalogirou, S. A., Solar thermal collectors and applications. *Prog. Energ. Combust.* **2004**, *30*,
876 (3), 231-295. DOI: 10.1016/j.pecs.2004.02.001.

877 105. Wong, L. T.; Mui, K. W.; Guan, Y., Shower water heat recovery in high-rise residential
878 buildings of Hong Kong. *Appl. Energy* **2010**, *87*, (2), 703-709. DOI:
879 10.1016/j.apenergy.2009.08.008.

880 106. Liu, L. B.; Fu, L.; Jiang, Y., Application of an exhaust heat recovery system for domestic hot
881 water. *Energy* **2010**, *35*, (3), 1476-1481. DOI: 10.1016/j.energy.2009.12.004.

882 107. McFeeters, R., Reuse of fermentation brines in the cucumber pickling industry. In
883 Environmental Protection Agency, O. o. R. a. D., Industrial Environmental Research Laboratory,
884 Ed. 1978; Vol. 1.

885 108. Romero Barranco, C. B. B., M.; Garcia Garcia, P.; Garrido Fernández, A., Management of
886 spent brines or osmotic solutions. *J. Food Eng.* **2001**, *49*, (2), 237-246. DOI:
887 [https://doi.org/10.1016/S0260-8774\(00\)00204-1](https://doi.org/10.1016/S0260-8774(00)00204-1)

888 109. Kammen, D. M.; Sunter, D. A., City-integrated renewable energy for urban sustainability.
889 *Science* **2016**, *352*, (6288), 922-8. DOI: 10.1126/science.aad9302.

890 110. World Health Organization. Progress on sanitation and drinking water: 2015 update and MDG
891 assessment. In 2015.

892 111. Zhang, L.; De Schryver, P.; De Gusseme, B.; De Muynck, W.; Boon, N.; Verstraete, W.,
893 Chemical and biological technologies for hydrogen sulfide emission control in sewer systems: a
894 review. *Water Res.* **2008**, *42*, (1-2), 1-12. DOI: 10.1016/j.watres.2007.07.013.

